



STUDY ON IMAGE DIAGNOSIS OF TIMBER HOUSES AFFECTED BY THE EARTHQUAKE UTILIZING DEEP LEARNING

H. Chida⁽¹⁾, N. Takahashi⁽²⁾

⁽¹⁾ Grad. Student, Dept. of Architecture, Tohoku University, hiroyuki-chida@pbd.archi.tohoku.ac.jp

⁽²⁾ Associate Professor, Tohoku University, ntaka@archi.tohoku.ac.jp

Abstract

The victims, who are affected by serious earthquake, often suffer the several difficulties such as long-term evacuation, due to consecutive aftershocks and reconstruction of their households. These difficulties were caused by various factors, especially delay of current inspection procedure of earthquake-damaged houses.

Several researches have been conducted in order to solve these issues. Image processing with deep learning has been evolved because particularly the image recognition has remarkably developed in recent years. In terms of timber houses, image classification is currently widely used, but it is difficult to adapt these methodologies into detailed inspections such as disaster certificate for insurance because image classification is good at qualitative damage assessment rather than quantitative one.

Thus, object detection and image segmentation have been attracting attention. This is because they have a potential for their automatic and speedy processing and enabling quantitative damage assessment. Actually, they were already used for infrastructures damage evaluation. In this study, the same technique is applied to the image diagnosis of timber houses damaged by earthquakes.

Firstly, a damage extractor was created and verified, which is based on semantic segmentation. The tagging all images in the database into four types of damage was carried out, that is crack and spalling in mortar exterior, crack in siding board, and crack in concrete basement. However, this database didn't work well in deep learning because of the lack of images and the bias of image feature values. Hence, chromakeying is employed and it enabled to improve deep learning accuracy, and the effectiveness of chromakeying to the deep learning database was also confirmed.

Secondly, a damage rate calculation process was built based on extracted damages. However, various noises were observed in extract results. Then in order to reduce these noises, pre- and post-image processing was employed and accuracy of damage extraction was improved. The quantitative damage assessment based on the guideline of damage assessment for earthquake insurance was conducted using damage extractors. And damage rate of some samples were also calculated to verifying the process.

Finally, for the improvement of image diagnosis, not only surface damage but also structural parameters should be considered, and the correlation between structural drift ratio and surface damage for Japanese timber houses was focused on. Although previous researches and limited experiments decides the correlation strictly, this is not enough for various conditions. Thus, the new experiments data were added to make the data improved. As a result, image diagnosis can estimate the range of structural maximum drift ratio according to the surface damage with non-structural components construction condition.

Keywords: Image diagnosis; Deep learning; Image processing; Timber house; Damage assessment



1. Introduction

The victims, who are affected by serious earthquake, often suffer the several difficulties such as long-term evacuation, due to consecutive aftershocks and reconstruction of their households. These difficulties were caused by various factors, especially delay of current inspection procedure of earthquake-damaged houses.

Several researches have been conducted in order to solve these issues. Image processing with deep learning has been evolved because particularly the image recognition has remarkably developed in recent years. In terms of timber houses, image classification is currently widely used, but it is difficult to adapt these methodologies into detailed inspections such as disaster certificate for insurance because image classification is good at qualitative damage assessment rather than quantitative one.

Thus, object detection and image segmentation have been attracting attention. This is because they have a potential for their automatic and speedy processing and enabling quantitative damage assessment. In this study, the same technique is applied to the image diagnosis of timber houses damaged by earthquakes. Then, the applicability of the image diagnosis to quantitative damage assessment was confirmed.

2. Image Database of Timber Houses Affected by Earthquakes

Image recognition using deep learning generally needs huge image database such as Image-Net [1]. However, it commonly takes an enormous amount of time and manpower to construct the image database. In order to simplify this construction process, transfer learning is widely used. The transfer learning transfers a pre-trained Convolutional Neural Network (CNN) model to an original CNN model which are made by original small image database. Then, the CNN model can get a rich knowledge for variety of image recognition.

However, in the case of collecting images of timber houses affected by earthquakes, it's not easy to collect the original small image database or could not be collectable. This is because these images are collectable only when a severe earthquake happen. Actually, trying the collecting images of damaged exterior walls from the past damage inspections in affected areas, these images were few and it was difficult to construct enough image database for deep learning. Thus, the data augmentation method was adopted to augment the image database which was made by real-damage images which were collected in the inspections. Then, a pseudo-damage image database was employed. This is because, the real-damage image database even took an enormous amount of time and manpower to select appropriate images for deep learning. Thus, the pseudo-damage image database was constructed from chroma-keying images, which made the construction process easy and speedy. And also, the pseudo-damage image database was more easily editable than real- damage image database.

2.1 Constructing image database and CNN models for damage extractors

To verify an applicability of pseudo-damage image database, leaning accuracy of two types of image database, which are real-damage image database and pseudo-damage one, was evaluated by two indicator such as mini-batch leaning accuracy and loss in the deep learning. Table 1 shows the employed CNN model cases which were consist of combination of pre-trained CNN models and CNN models.

Table 1 – Cases of CNN models

Case names	SV16	SV19	DLR18	DLR50	DLM	DLX	DLIR
CNN models	SegNet		DeepLabv3+				
Pre-trained CNN models	VGG16	VGG19	ResNet18	ResNet50	MobileNetv2	Xception	InceptionResNetv2



In this verification, six image databases for each kind of damage such as real mortar cracks (RMC), chromakeying/pseudo mortar cracks (CMC), real mortar spalling (RMS), chromakeying/pseudo mortar spalling (CMS), real siding board cracks (RBC), and chromakeying/pseudo siding board cracks (CBC) were used for each CNN model cases. Therefore, forty-two cases which consist of seven CNN models and six image databases were examined. These cases were evaluated by indication of learning accuracy and loss. Fig. 1 shows an example of results of learning accuracy and loss. The higher learning accuracy, the more successful deep learning, and the closer the learning loss is to zero, the more successful deep learning. Thus, all cases were evaluated by the indicator, and it was confirmed that the all cases had enough learning accuracy.

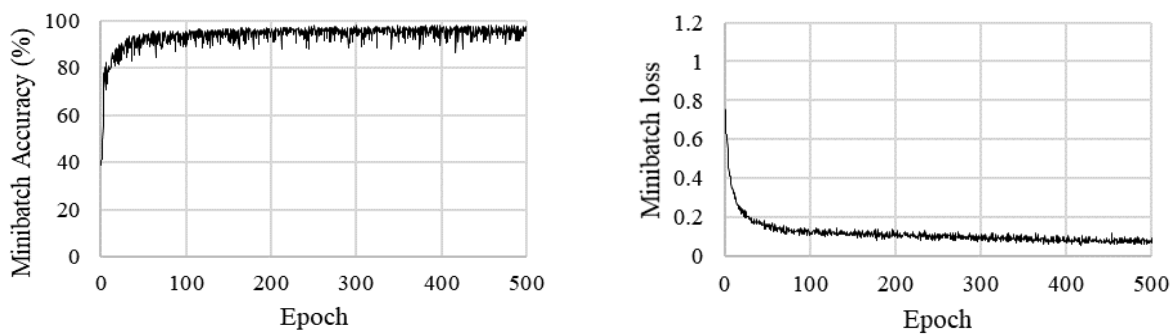


Fig. 1 – Examples evaluation with learning accuracy and loss (Case of SV19/RMC)

After evaluation of the learning accuracy, recognition accuracy of each cases was evaluated by damage extraction results of 100 test images. Fig. 2 shows indicator of the recognition accuracy such as recall and precision. Recall is index in order to evaluate recognition omissions, and precision is index in order to evaluate false recognition. These indexes are calculated from Eq. (1) and Eq. (2).

Table 2 – Metrics of data prediction

		Ground Truth	
		Positive	Negative
Predicted	Positive	True Positive	False Positive
	Negative	False Negative	True Negative

$$Recall = TP / (TP + FN) \quad (1)$$

$$Precision = TP / (TP + FP) \quad (2)$$



Table 3 shows examples of evaluation results of recall and precision. When the value of recall is closer to 1, recognition omissions area is decreased. When the value of precision is closer to 1, the false recognition area is also decreased. In terms of damage extraction, recognition omissions which cause underestimate of damage assessment should not be allowed. Thus, recall was evaluated intensively to make damage extractor which can recognize whole damage area. And also, in order to prevent false recognition area, precision was evaluated as a second indicator.

After evaluating recall and precision of each CNN model cases, the best result case of CNN model for each damage database is selected except for RBC. Table 4 shows the summary of employed CNN models.

Table 3 – Examples of evaluation with recall and precision

CNN cases	SV16/CMC	SV16/CMS	SV16/CBC
Original images			
Ground truth			
Predicted results			
Evaluation images			
Recall	0.960890	0.781363	0.762427
Precision	0.385761	0.913714	0.667609



Table 4 – Summary of employed CNN models

Damage types	Image database	Model names	CNN models	Pre-trained CNN models	Average of recall	Average of precision
Mortar crack	Real damage	DLR50/RMC	DeepLabv3+	VGG16	0.745	0.190
	Chromakey damage	SV19/CMC	SegNet	VGG19	0.748	0.195
Mortar spalling	Real damage	SV16/RMS	SegNet	ResNet18	0.799	0.967
	Chromakey damage	DLR50/CMS	DeepLabv3+	ResNet50	0.746	0.948
Board crack	Real damage	—	—	—	—	—
	Chromakey damage	DL50/CBC	DeepLabv3+	Xception	0.566	0.274

These CNN models had the maximum values of average recall and precision of each models evaluated by 100 test images. However, the CNN model for RBC didn't work well, and its recall and precision were zero. This is because, the surface of siding board is often contaminated and cracks on the siding board cannot see clearly. Thus, the chromakeying/pseudo damage model of siding board crack (CBC) was only adopted.

2.2 Evaluation of CNN models based on damage extraction results

Based on the damage extraction results of each CNN models which applied to the photos of Kumamoto earthquake reconnaissance in 2016, each CNN models were evaluated and compared. Fig. 2 shows the comparison of damage extraction results for each CNN models.



Fig. 2 – Comparison of damage extraction results



CNN models for chromakeying/pseudo damage image database can extract the damage more accurate rather the CNN models for real damage image database. Thus, SV19/CMC, DLR50/CMS, and DLR50/CBC were adopted for damage extractors in the following discussion.

3. Damage Evaluation Method Based on Damage Extraction Results

Before damage evaluation, the noises such as plants and wires in the damage extraction results shown in Fig. 2 were removed by using pre- and post-image processing algorithm. Then, the damage rate calculated based on the damage extraction results.

3.1 Pre- and post-image processing for noise elimination

During the pre-image processing, graph cut technique [2] was applied to damage extraction results which were extracted by semantic segmentation. Fig. 3 shows the example process of graph cut processing. The graph cut can segment area such as building and background. In this pre-image processing, the noises in the background were eliminated. However, some noises in the foreground on the building remained, and post-image processing was applied to the results. During the post-image processing, area limitation and Hough transformation [3] denoised the foreground noises. Fig. 4 shows the example of pre- and post-image processing.

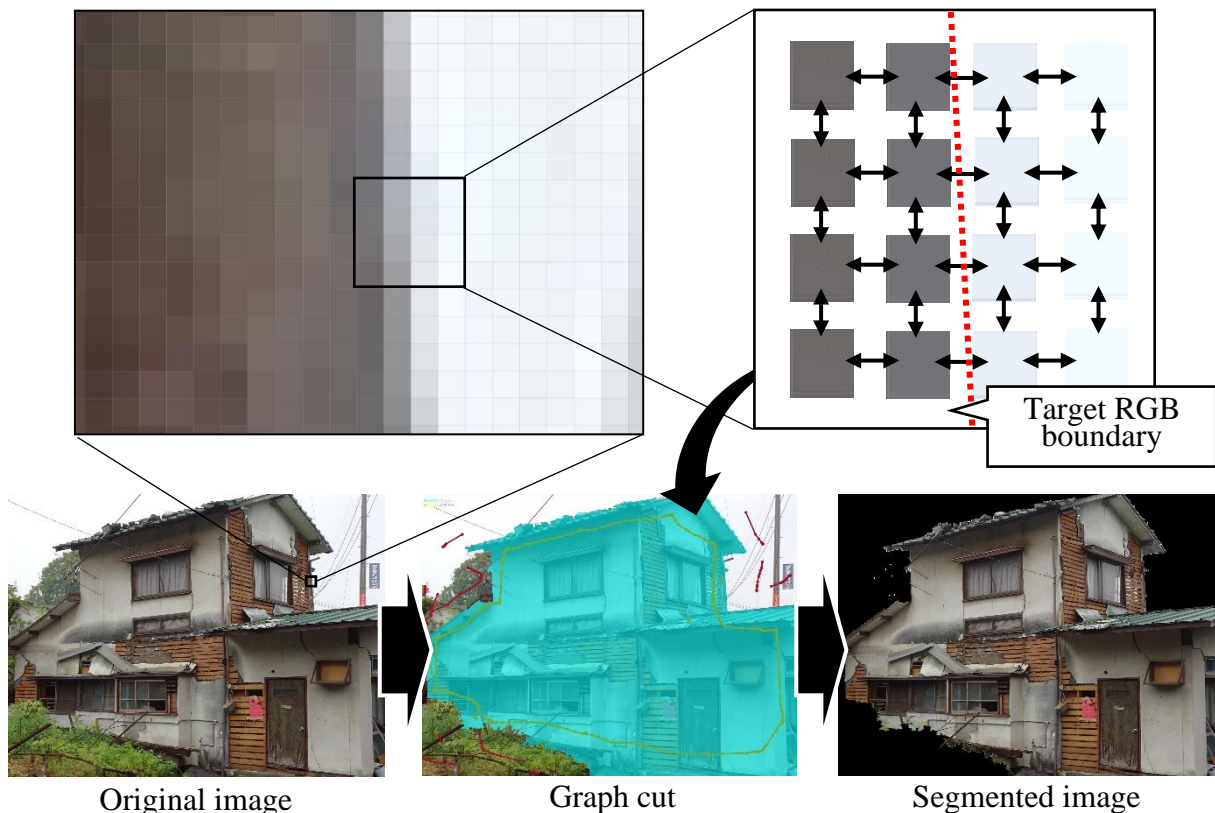


Fig. 3 –Example of graph cut processing

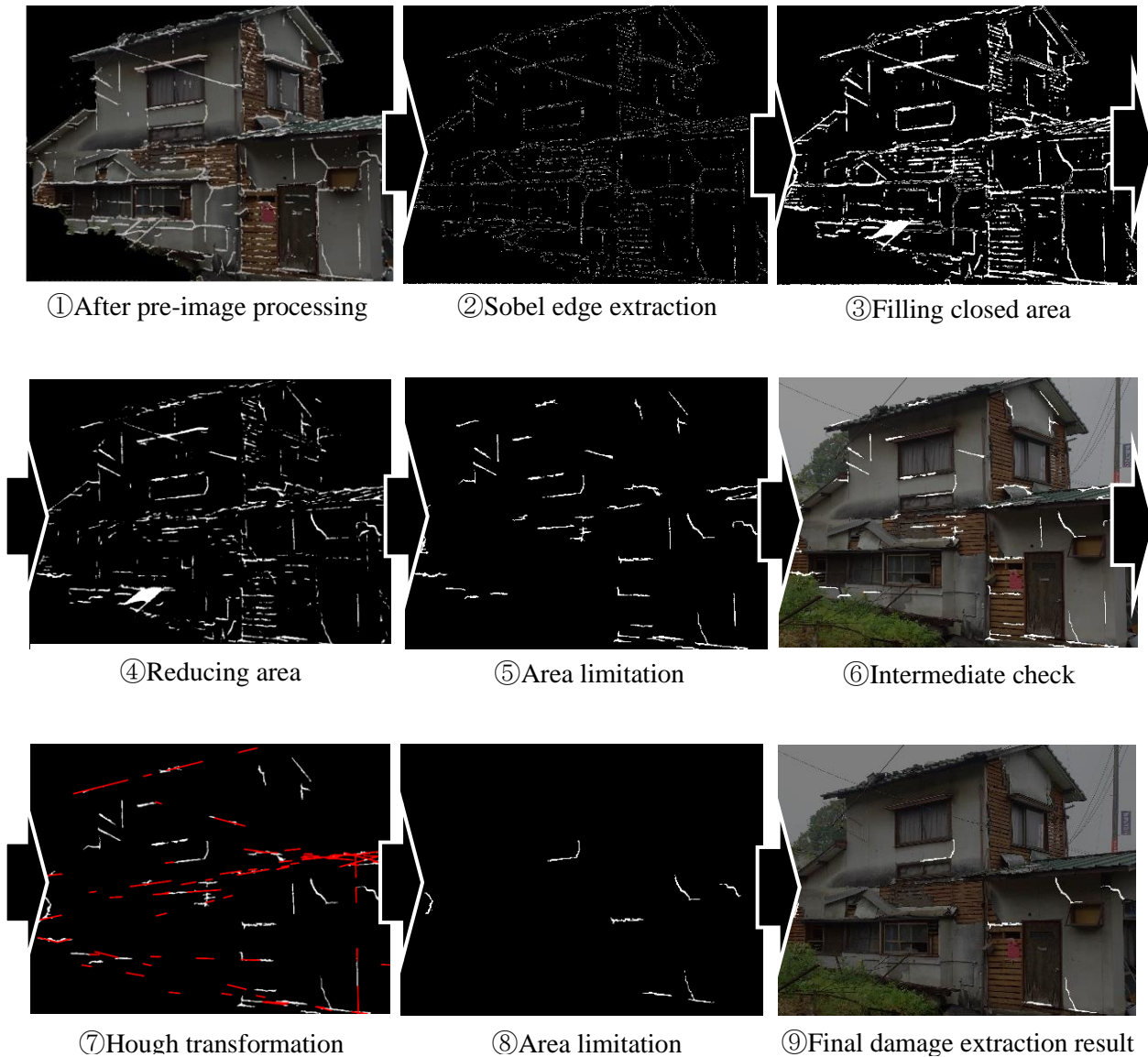


Fig. 4 –Example of pre- and post-image processing

In the post-image processing algorithm, the edge of damage extraction area which was extracted by semantic segmentation and pre-image processing was firstly extracted by Sobel edge extraction method [4]. Then, the closed area was filled and grouped, and deleting 1 pixel of edge from each filled area groups. This is because, Sobel edge extraction usually made area thicker than original area. After that, some noises remain. Thus, noises were eliminated by considering the area ratio which divide the extracted area into crack area and noise area. At the intermediate check, there were still some noises such as wires, eaves and window frames which were straight line. Then, the linear noises were denoised by Hough transformation. And finally, the remained noises were eliminated by area limitation again.

Using only semantic segmentation, the correct damage area was not extracted but a lot of noises were extracted with damage area. After the pre- and post-image processing were applied to the noisy images, its applicability was confirmed.



3.2 Quantitative damage evaluation method based on damage extraction results

For damage evaluation, the following equations shown in Eq. (3) to (5) were expressed by the damage assessment guideline for earthquake insurance [5].

$$DR_{ins} = \sum_i \left(\frac{dw_i}{aw_i} \times \frac{aw_i}{Aw} \right) = \sum_i (\alpha_i \times \beta_i) \quad (3)$$

$$\alpha_i = \frac{dw_i}{aw_i} \quad (4)$$

$$\beta_i = \frac{aw_i}{Aw} \quad (5)$$

where, DR : damage rate of exterior wall damage, dw_i : damage area on i^{th} side of wall, aw_i : wall area on i^{th} side of wall, Aw : whole wall area, α_i : damage rate of i^{th} side of wall, β_i : area rate of i^{th} side of wall

In this paper, Eq. (4) was used for damage assessment of a single side of wall. To verify the validation of damage calculation results, the observed results of damage rate which were obtained from visual inspection by three persons. Table 5 shows the calculation results based on the extraction results with pre- and post-image processing. Where, the 1st, 2nd, 3rd: human-observation results, ERh : maximum human error rate among three persons' results, ERd : maximum diagnosis error rate between three persons' results and image diagnosis results.

In the first case, ERh was nearly equal to ERd . Therefore, it was considered that the image diagnosis could be done correctly. On the contrary, in other cases, there were large errors between damage rate calculated by human and by image diagnosis. Particularly, the third case and the fifth case had large errors. This was because, on the exterior walls, there were some minor cracks, which were difficult to find out from low resolution images. Moreover, in the second case and the fourth case, damage rate calculated by image diagnosis was lower than human-observation values. This was because some damages were covered by green-plants and trees, which made the damage invisible. Then, the invisible damages were not extracted by image diagnosis, but could be estimated and considered for damage calculation by human. Thus, there were some errors between the image diagnosis results and human calculation results.

However, in the fourth case, it was confirmed that human error also could be happened because of covering damage and image resolution. These human errors could be happened in the range up to approximately 25%. Thus, considering the range of human error rate, image diagnosis results in the first, second and fourth case could be considered roughly equal to human-observation results. Thus, it was confirmed that when the damage rate calculated by image diagnosis was over 65%, the image diagnosis could be done correctly with accuracy equal to the human visual calculation of damage rate.



Table 5 – Results of damage rate calculation

No.	1	2	3	4	5
Original images					
Extraction results					
α_i	A side: 79.5% B side: 98.8%	71.4 % (2F)	27.5% (1F) 8.8% (2F)	64.3% (1F) 0% (2F)	23.3% (2F)
1st	A side: 71.6%, B side: 98.7%	81.7% (2F)	15.2% (1F) 42.2% (2F)	65.3% (1F) 0% (2F)	34.5% (2F)
2nd	A side: 70.3% B side: 96.9%	81.8% (2F)	13.1% (1F) 48.2% (2F)	86.9% (1F) 0% (2F)	42.0% (2F)
3rd	A side: 89.8% B side: 98.2%	81.1% (2F)	13.7% (1F) 47.1% (2F)	83.4% (1F) 0% (2F)	34.5% (2F)
ER_h	A side: 21.7% B side: 1.8%	0.9%	13.8%(1F) 12.4% (2F)	24.9% (1F) 0% (2F)	17.9%
ER_d	A side: 11.4% B side: 1.9%	12.7%	52.4%(1F) 81.7% (2F)	26.0% (1F) 0% (2F)	44.5%

From the above results, the image diagnosis system can be proposed as shown in Fig. 5. In this paper, after damage extraction and denoising, damage rate could be correctly and quantitatively calculated in the range over 65%.

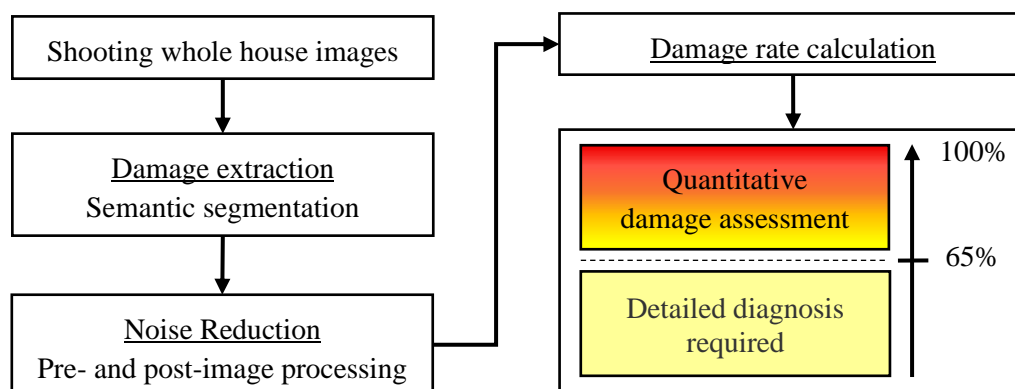


Fig. 5 –System of damage rate calculation based on image diagnosis



4. Estimation of Structural Drift Ratio Based on Surface Damage Image Diagnosis

In the image diagnosis system, the damage which appears on the exterior walls was assessed. This damage assessment results could be used for calculating repair cost and evaluation of repair performance. On the other hand, the seismic performance could not be assessed by using only the image diagnosis system without structural earthquake response. Thus, in this chapter, it was considered that combining the image diagnosis system and structural earthquake response estimation method.

In the current inspection [6] in Japan, estimation methodology as shown in Table 6 in order to estimate experienced maximum drift ratio and residual seismic performance of timber houses is often used. The estimation of experienced maximum drift ratio is conducted based on inspection of superficial damages such as exterior wall damage and interior wall damage. Since there is a possibility of upgrading of image diagnosis system, the applicability was examined.

Table 6 – Estimation methodology of the current inspection in Japan [6]

		Type of exterior wall	
		Mortar	Siding board
Maximum experienced drift ratio (rad.)	~1/300	Minute cracks around opening corner	—
	~1/200	Cracks around opening corner	—
	~1/120	Expansion of cracks around opening corner	Nails are about to come off
	~1/60	Cracks around the opening without corner	Cracks around opening corner
	~1/45	Expansion of cracks around opening without corner	Expansion of cracks around opening corner / A board is about to come off
	~1/20	A crack on flat parts of wall without opening	A crack around the corner of opening goes up and down
	Over 1/20	cracks on flat parts of wall without opening	Cracks around the corner of opening go up and down

Moreover, the estimation methodology was proposed mainly for Japanese timber houses which were built according to the seismic standard before 2000. Because of the revision of Japanese seismic standard for timber houses in 2000, the estimation methodology needs to be improved. Therefore, in order to apply the methodology to houses which were built after 2000, the methodology was upgraded by the previous experimental results [7][8] and experimental results of full-scale timber specimens [9][10] in this research.

Fig. 5 shows the upgraded estimation method. The estimation of drift ratio of timber houses based on the current seismic standard houses was smaller than that of timber houses based on the old standard. This was because, the value of stiffness and maximum strength of timber houses based on the current standard became higher than that of old standard. Therefore, it was suggested that when the estimation method based on the old standard was applied to the timber houses based on the current standard, the estimation results could be higher than actual drift ratio.

Table 7 shows the estimation results using the image diagnosis results. It was confirmed that the maximum experienced drift ratio of each images was estimated. And also, using meta-data, which was the difference of construction years, it was suggested that the estimation results could be obtained more appropriately.

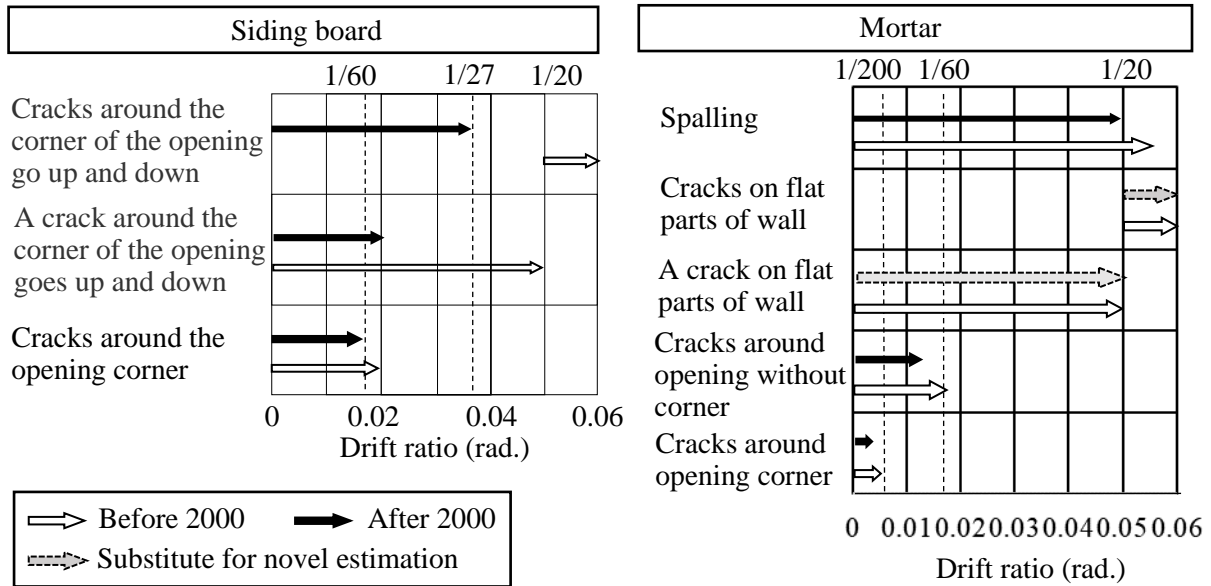


Fig. 6 –Drift ratio estimation classified by construction year

Table 7 – Drift ratio estimation results

No.	1	2	3	4	5	
Original images						
Extraction results						
Drift ratio estimation	Before 2000	Up to 1/15 rad.	Up to 1/15 rad.	Up to 1/60 rad.	Up to 1/15 rad.	Up to 1/27 rad.
	After 2000	Up to 1/20 rad.	Up to 1/20 rad.	Up to 1/75 rad.	Up to 1/20 rad.	Over 1/20 rad.



5. Concluding remarks

In this paper, quantitative seismic damage assessment method based on image diagnosis utilizing deep learning and pre- and post-image processing was proposed and verified. As a result, the following three findings were revealed.

- (1) The real image database was not always required for construction of image database for deep learning, but pseudo-damage image database made by chroma-keying could be effectively used for deep learning, which made the damage extractor with enough learning and recognition accuracy.
- (2) The quantitative seismic damage assessment could be conducted based on image diagnosis results. The threshold value for appropriate damage quantification was over 65% damage rate.
- (3) Based on image diagnosis results, the range of experienced maximum drift ratio was estimated. It was suggested that these estimation results could be additional data for quantitative damage assessment for Japanese timber houses.

6. References

- [1] Krizhevsky A., Sutskever I., Hinton G. (2017): ImageNet Classification with Deep Convolutional Neural Networks, *Communications of the ACM*, Vol. 60, No. 6, pp.84-90
- [2] Oyeboode K., Du S., van Wyk B., Djouani K. (2019): Investigating the Relevance of Graph Cut parameter on Interactive and Automatic Cell Segmentation, *Hindawi Computational and Mathematical methods in Medicine*, Vol. 2018, Article ID 7396910
- [3] Duda R., Hart P. (1971): Use of Hough Transformation to Detect Lines and Curves in Pictures, *Graphics and Image Processing*, Vol. 15, No. 1, pp. 11-15
- [4] Kanopoulos N., Vasanthavada N., Baker R. (1988): Design of Image Edge Detection Filter Using the Sobel Operator, *IEEE Journal of Solid-state Circuits*, Vol. 23, No. 2, pp. 358-367
- [5] The General Insurance Association of Japan (2010): Damage Assessment Guideline for Earthquake Insurance, The General Insurance Association of Japan, (in Japanese)
- [6] Association of Japan Architectural Disaster Prevention (2016): Disaster damage classification criteria and restoration technical guidelines for earthquake-damaged buildings (in Japanese)
- [7] Oki, Y. and Kajikawa, H. (2014): A study on the earthquake damage evaluation that paid its attention to the story drift of the building and relations of the finishing materials damage and the structure damage (Part.1 Investigation of a Study of the Past), Summaries of Technical Papers of Annual Meeting, *Architectural Institute of Japan*, Structures-III, pp.581-582 (in Japanese)
- [8] Sato, M. et al. (2016): A study on the earthquake damage evaluation that paid its attention to the story drift of the building and relations of the finishing materials damage and the structure damage.(Part.3 A result of experiment about a relation between horizontal-displacement and damage of finishing-materials.), Summaries of Technical Papers of Annual Meeting, *Architectural Institute of Japan*, Structures-III, pp.543-544 (in Japanese)
- [9] Nishi, R., Uwadan S., Nagae, T., Takahashi T., Kajiwaru K., Yamada S., Kashiwa H., Hayashi K., Inoue T. (2018): Performance Assessment for a Test Specimen Extracted from the Lower Part of a Three-Story Dwelling Part.1 Damage Process and Hysteretic Behaviors in the Force-Deformation Relation, 91st Research Presentations in Hokkaido (*Transactions of AIJ*), pp.167-170 (in Japanese)
- [10] Inoue T., Yamada S., Kashiwa H., Hayashi K., Nagae T. (2018): E-Defense test on functionality of three-story residential houses including underground pipe lines (Metropolitan resilience PJ) Part.1 Overview of the project and perspectives of the E-Defense test, Summaries of Annual meetings, *Architectural Institute of Japan*, Structures-II, pp.231-232 (in Japanese)